REGAL International Program: Analysis of experimental data for depletion code validation

J. Eysermans, M. Verwerft, K. Govers, Raphaelle Ichou, G. Ilas, U. Meryturek, N. Messaoudi, P. Romojaro, N. Slosse

Annals of Nuclear Energy 172 (2022) 109057

Contents lists available at ScienceDirect

Annals of Nuclear Energy

journal homepage: www.elsevier.com/locate/anucene

REGAL International Program: Analysis of experimental data for depletion code validation

J. Eysermans [a,b,*], M. Verwerft [b], K. Govers [b,1], R. Ichou [c], G. Ilas [d], U. Meryturek [d], N. Messaoudi [b], P. Romojaro [b], N. Slosse [e]

[a] MIT, Cambridge, Massachusetts, USA, 77 Massachusetts Ave, Cambridge, MA 02139, United States
[b] Belgian Nuclear Research Centre (SCK CEN), Boeretang 200, 2400 Mol, Belgium
[c] Institut de Radioprotection et de Sûreté Nucléaire (IRSN), 31 avenue de la Division Leclerc, 92260 Fontenay-aux-Roses, France
[d] Oak Ridge National Laboratory, Oak Ridge 37831, TN, United States
[e] Tractebel Engineering S.A., Boulevard Simon Bolivar 34, 1000 Brussels, Belgium

ARTICLE INFO

Article history:
Received 20 December 2021
Received in revised form 20 February 2022
Accepted 3 March 2022
Available online 22 March 2022

Keywords:
Reactor Physics
Depletion
Predictive modeling
Gadolinia fuel

ABSTRACT

The Rod-Extremity and Gadolinia AnaLysis (REGAL) Program is a joint international effort to expand the nuclide inventory experimental data for irradiated nuclear fuel, with a specific focus on addressing two challenging needs associated with the characterization of modern, high duty, nuclear fuel. The first challenge is filling the gaps in experimental nuclide inventory data for gadolinia (UO_2–Gd_2O_3) fuel rods. The huge absorption cross sections of Gd-155 and Gd-157 in the Gd dopant in these rods lead to atypical spatial self-shielding patterns and have an impact on the neutronic environment within the fuel assembly compared to regular UO_2 fuel rods. The second challenge is investigating the impact of burnup gradients at rod extremities on fuel composition and neutron leakage, to provide relevant experimental data for assessing computational capabilities to model such impact. A benchmark has been defined as a first step in the development of best-estimate models in the preliminary phase of the experimental data evaluation. Comparison of experimental results obtained in Phase I of the program for two measured pressurized water reactor (PWR) samples, one UO_2 and one UO_2–Gd_2O_3 sample, with calculated results obtained with different computational tools based on the defined benchmark are presented and discussed.

1. Introduction

High-quality experimental data of nuclide inventories in spent nuclear fuel are critical for the validation of computational tools and associated nuclear data that are used to simulate the nuclide transmutations and decay in nuclear fuel during and after irradiation. They provide the basis for evaluating the bias and uncertainty in code predictions of key metrics of importance to back-end fuel cycle applications, like decay heat, as well as full-core reactor safety analyses. This validation basis must be continuously reassessed and expanded to address changes in validation needs and keep pace with changes in operation and fuel designs and characteristics for current and future commercial reactors.

High-accuracy measurements of nuclide inventories can be obtained by destructive radiochemical assay (RCA) experiments. These types of experiments require complex analytical methods (i.e., for sample preparation, chemical separation, spectrometry), specialized instruments and expertise, state-of-the-art experimental laboratories, and facilities for handling and measuring irradiated nuclear fuel. Experimental programs for nuclide inventory measurements are challenging endeavors which, as demonstrated by past international efforts, can be successfully performed through collaborative efforts, benefitting from diverse expertise and capabilities across institutions in various countries (Boulanger et al., 2004; Baeten et al., 2002).

The Rod-Extremity and Gadolinia AnaLysis (REGAL) Program is a joint international effort to expand the experimental nuclide inventory data for irradiated nuclear fuel. It specifically focuses on addressing two challenging needs associated with the characterization of modern, high duty, nuclear fuel. The first challenge is filling the gaps in experimental nuclide inventory data for gadolinia (UO_2–Gd_2O_3) fuel rods. The huge absorption cross sections of Gd-155 and Gd-157 in the gadolinium (Gd) dopant in these rods lead to atypical spatial self-shielding patterns and have an impact on the neutronic environment within the fuel assembly compared to regular UO_2 fuel rods. Secondly, the program is investigating the

* Corresponding author.
[1] Presently at Federal Agency for Nuclear Control (FANC), Rue du Marquis 1 bte 6A, B-1000 Brussels, Belgium.

https://doi.org/10.1016/j.anucene.2022.109057
0306-4549/

impact of burnup gradients at rod extremities on fuel composition and neutron leakage, to provide relevant experimental data for assessing computational capabilities to model such an impact.

Gadolinia (UO_2–Gd_2O_3) fuel rods are currently used routinely in the nuclear industry. The gadolinium acts as a burnable poison to control the reactivity evolution at the beginning-of-life of the fuel assembly and optimizes fuel performance during operation (Hesketh et al., 2020). While earlier designs of gadolinia rods had Gd_2O_3 loadings of up to 5–6% and natural uranium or uranium enrichments lower than that of regular UO_2 rods within the same fuel assembly (Manzel and Dorr, 1980), modern designs are characterized by Gd_2O_3 loadings up to 10% and uranium enrichment closer to that of the UO_2 rods in the assembly.

The local inhomogeneities induced by rod extremities or burnable poison rods are challenging for the prediction by neutron transport codes and coupled depletion codes. The assessment of their predictive qualities relies on relevant high-quality experimental data which are scarce in the open literature. The REGAL project aims to fill this gap by performing high-quality radiochemical analyses on a one-cycle irradiated gadolina fuel rod and two 'high-duty' UO_2 sibling rods, all irradiated in the Tihange 1 (Belgium) pressurized water reactor (PWR). In the framework of REGAL, blind cross-checks on quasi-identical samples are planned, with multiple highly reputable radiochemical laboratories. These cross-check analyses will allow improving the measurement uncertainties and increase confidence in the reported results. Moreover, the nuclide inventory information averaged over the fuel pellet that is obtained by destructive radiochemical analysis will be complemented by a spatially resolved local analysis using Secondary Ionization Mass Spectrometry (SIMS) and Electron Probe Micro Analysis (EPMA) to describe the radial distribution of nuclides in the fuel pellet.

SFCOMPO, the world's largest database (OECD-NEA, 2017; Michel-Sendis et al., 2017) of measured nuclide inventories in spent nuclear fuel, provides RCA data for 750 samples selected from fuel irradiated in 44 reactors of different types, and with measurement data for over 90 nuclides important to the reactor and back-end fuel safety applications. Albeit extensive and covering a large space of fuel characteristics, the database is limited in data for gadolinia fuel. Only 49 UO_2–Gd_2O_3 samples selected from fuel irradiated in one PWR and in five boiling water reactors (BWRs) are present in SFCOMPO. Only 5 of these 49 samples include measurements for Gd-155 and Gd-157. Two of these five samples, from Fukushima-Daini-1 (Japan) BWR fuel and with burnups of 28 and 54 GWd/t_{HM}, were selected from the same fuel rod with an initial 5% Gd loading. The other three samples from the Ohi-2 (Japan) BWR, were selected from two fuel rods with 6% Gd initial loading and had burnups in the 21–29 GWd/t_{HM} range. The REGAL samples fill existing data gaps for lower burnups of less than 15 GWd/t_{HM}, of high relevance to peak reactivity in BWRs and to optimize fuel performance during operation.

The REGAL Program is coordinated by SCK CEN, the Belgian Nuclear Research Centre, who also coordinated earlier successful international spent fuel assay programs such as MALIBU (Boulanger et al., 2004), and participated actively in the ARIANE program (OECD-NEA, 2011). Phase I of REGAL, which formally started in 2016 and was completed in 2021, included measurements of ten spent fuel samples, five from a UO_2 rod and five from a gadolinia rod. The REGAL partners at the start of Phase I included, in addition to the SCK CEN lead, participants from ENGIE and Institut de Radioprotection et de Sûreté Nucléaire (IRSN) in France, and Oak Ridge National Laboratory (ORNL) in the United States. Later, other French institutions joined the program: CEA, EDF, and FRAMATOME. Phase II of REGAL, initiated in 2021, will include cross-checks of selected samples at different measurement laboratories, measurements of radial distributions within the fuel rod of nuclide inventories, and an expanded analysis matrix.

Comparison of experimental results obtained in Phase I for two of the measured samples (one UO_2 and one UO_2–Gd_2O_3) with the corresponding calculated results obtained with different computational tools are the subject of this paper. The experimental data are summarized in Section 2, followed by a description in Section 3 of a benchmark model proposed as a first step in developing best estimate models for the analyses of the REGAL samples. Computational models are presented in Section 4, and analysis results in Section 5. Discussion of the results and concluding remarks are provided in Section 6.

2. Experimental data

The fuel samples measured in the REGAL Phase I were taken from three fuel rods: two UO_2 fuel rods from the same assembly and one gadolinia fuel rod from another assembly. Both assemblies were irradiated in the Tihange 1 PWR. Each of the UO_2 rods had an estimated rod-average burnup of approximately 50 GWd/t_{HM} and were irradiated in the reactor for two consecutive cycles. The gadolinia rod, irradiated for only one cycle, had an estimated rod-average burnup of approximately 12 GWd/t_{HM} (Govers et al., 2015). The main characteristics of these rods in comparison with those rods that were the subject of investigations under the ARIANE and MALIBU programs are presented in Table 1. As seen, the REGAL technical scope adds to and complements that of the two previous efforts. The characteristics of the rods considered under REGAL, the focus on gadolinia fuel and special attention to rod extremities, make the experimental database more applicable to modern fuel assemblies and reactor operation (longer fuel cycles, smaller number of cycles to achieve higher burnup, and the inclusion of integral burnable absorbers such as gadolinia rods with a high Gd loading).

RCA measurements performed under REGAL Phase I were based on state-of-the-art experimental techniques and instruments and involved Isotope Dilution Thermal Ionisation Mass Spectrometry (ID-TIMS), Inductively Coupled Plasma Mass Spectrometry (ICP-MS), and α- and γ-spectrometry. The nuclides measured for the two fuel samples that are the subject of detailed analysis and discussion in this paper are listed in Table 2. The relative experimental uncertainties for the measured nuclides discussed in this paper are included in the table and account for the combined uncertainty due to sampling, weighing, dilution, and nuclide inventory analysis. They are expressed at the 95% confidence level. For uranium and plutonium isotopes, the sampling and dilution uncertainties generally dominate the overall uncertainty. The table also notes the nuclide importance to key metrics for reactor safety and back-end fuel cycle applications: Burnup Credit (BC), Radiological Safety (RS), Waste Management (WM), and Burnup Indicator or related (BI) (OECD-NEA, 2011).

3. Benchmark based on REGAL experimental data

A computational benchmark has been defined as a first step towards the development of best-estimate models for simulating the irradiation and decay history of the measured samples to calculate the nuclide inventories in these samples. This approach ensures consistency among the participants in the preliminary phase of the experimental data evaluation and minimizes potential sources for any differences in the calculated inventories that would be due to the use of various simplifications and assumptions necessary for the various computational tools used in the analyses. The primary simplifications and assumptions of this benchmark model are discussed in this section. Nevertheless, small differences

Table 1
Main characteristics for PWR UO_2 fuel rods in ARIANE, MALIBU, and REGAL international programs (Govers et al., 2015; OECD-NEA, 2011).

Program	ARIANE	MALIBU	REGAL	
Fuel type in measured rod	UO_2	UO_2	UO_2	UO_2–Gd_2O_3
Number of cycles	3 and 5	4	2	1
Cycle length (months)	12	12	18	18
Assembly	15 × 15 (without Gd)	15 × 15 (without Gd)	15 × 15 (with Gd)	15 × 15 (with Gd)
Rod-average burnup (GWd/t_{HM})	30, 50 and 60	50 and 70	50	12
Fuel enrichment (wt.% U-235/U)	3.5 and 4.2	4.3	4.25	2.0
Fuel Gd content (wt.% Gd_2O_3/UO_2–Gd_2O_3)	no Gd	no Gd	no Gd	10.0

Table 2
Measured nuclides and experimental techniques.

Nuclide	Technique	Application[a]	Exp. unc. (%) UO_2 sample	Exp. unc. (%) UO_2–Gd_2O_3 sample
U-234	ID-TIMS	BC, WM	0.8	4.2
U-235	ID-TIMS	BC, WM	0.7	1.0
U-236	ID-TIMS	BC, WM	0.7	1.0
U-238	ID-TIMS	BC, WM	0.7	1.0
Pu-238	ID-TIMS	BC, RS, WM	1.6	1.0
Pu-239	ID-TIMS	BC, RS, WM	0.6	1.0
Pu-240	ID-TIMS	BC, RS, WM	0.6	1.0
Pu-241	ID-TIMS	BC, WM	0.6	1.0
Pu-242	ID-TIMS	BC, WM	0.7	1.0
Am-241	γ-spec	BC, RS, WM	5.7	5.1
Cm-244	α-spec	BC, WM	8.0	5.1
Cs-134	γ-spec	RS	5.1	4.1
Cs-137	γ-spec	BI, RS, WM	4.4	4.1
Nd-143	ID-TIMS	BC	2.5	2.3
Nd-144	ID-TIMS	BI	2.3	2.3
Nd-145	ID-TIMS	BC, BI	2.3	2.3
Nd-146	ID-TIMS	BI	2.3	2.3
Nd-148	ID-TIMS	BI	4.4	4.4
Nd-150	ID-TIMS	BI	8.9	8.9
Gd-155	ID-TIMS	BC	n.a.[b]	3.3
Gd-157	ID-TIMS	BC	n.a.[b]	1.9

[a] Burnup Credit (BC), Radiological Safety (RS), Waste Management (WM) and Burnup Indicator or related (BI).
[b] Not applicable (not measured).

in the implementation of the benchmark description among the codes are still expected, due to inherent differences in methods and capabilities of the individual codes considered, as will be discussed in Section 4. Therefore, the benchmark definition focuses on ensuring consistency among the codes rather than providing the best-estimate description of the fuel irradiation, the latter which ultimately depends on the code utilization itself. The adequacy of the proposed benchmark model is assessed by comparing the calculated nuclide inventories with the corresponding experimental data.

Fuel properties and conditions during irradiation are available in data books that are based on data provided by the fuel vendor and reactor operator. In the following, the name of the samples is referred to as D05 and E14, corresponding to the rod from where the UO_2 and UO_2–Gd_2O_3 samples have been taken respectively. The data books available for the fuel rods D05 and E14 have served as the basis for the benchmark model definition, which required simplifications that took into account the computational aspects of the modeling and compatibility of implementation among the various codes.

3.1. Operating history of the fuel rods

The D05 and E14 rods were irradiated in the Tihange 1 PWR reactor in Belgium in different reactor cycles, therefore their operational history and irradiation characteristics differ significantly. The operational history in terms of linear heat production (W/cm) and burnup accumulation (GWd/t_{HM}) at sample elevation are shown in Fig. 1. These quantities are based on neutronic and thermal balance reactor calculations.

Rod D05 is a nominal-enriched UO_2 type fuel, irradiated in two cycles between 1998 and 2001, for a total duration equivalent to almost 1000 effective full power days (EFPD). At the end of the first cycle, a stretch-out was performed to prolong the cycle by reducing the power and average core temperatures to maintain core criticality. The estimated burnup at sample elevation is 54.3 GWd/t_{HM}. On the other hand, rod E14 is a gadolinia rod and was irradiated for a single cycle for approximately 450 EFPD between 2002 and 2004. From reactor core calculations, the burnup for the measured sample from this rod is estimated to be 14.2 GWd/t_{HM}. Both samples were taken from the central part of their respective fuel rods, corresponding to the flat burnup zone of the core.

During the reactor cycle, core criticality is maintained by boron dilution in the primary water moderator, with an initial concentration of approximately 1200 ppm which is gradually decreased towards the end of the cycle. Furthermore, the operational control rods are gradually withdrawn from the core to control reactivity, shifting the core power elevation upwards. The mean coolant pressure and temperature remain constant except during the stretch-out period.

3.2. Assembly and fuel data

Although rods D05 and E14 were irradiated in different reactor cycles, they were hosted in the same fuel assembly type. A sketch of the fuel assembly indicating the positions of the D05 and E14 rods is shown in Fig. 2. It is a standard 15 × 15 assembly lattice

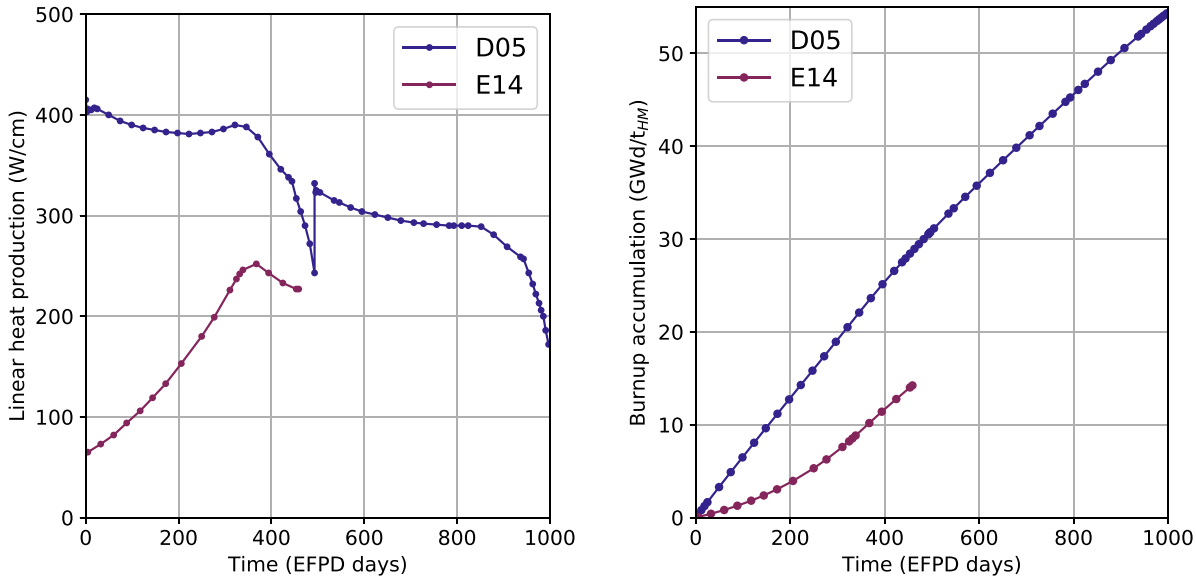

Fig. 1. Irradiation history at sample elevation: calculated linear heat production and burnup accumulation during irradiation in the Tihange 1 reactor for D05 and E14 samples, based on neutronic and thermal balance reactor calculations.

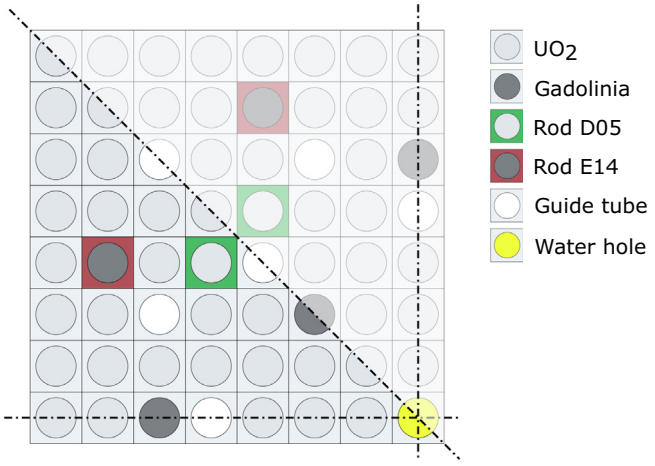

Fig. 2. Geometrical model of the 15 × 15 fuel assembly, with the top-left quadrant shown and with 1/8 symmetry indicated. Rods D05 and E14 are marked in green and red respectively, with their symmetric positions in the assembly.

containing 188 UO_2 rods and 16 UO_2–Gd_2O_3 rods, 20 guide tubes, and one central lattice location containing water for instrumentation insertion. Typical rod and assembly pitch values are used, evaluated at hot core conditions, and taking into account the thermal expansion of the assembly and spacer grids. All fuel rods have identical dimensions and the M5 material is used for cladding. The guide tube and rod dimensions are evaluated at cold conditions.

The as-manufactured diameter is considered when modeling the fuel pellets, therefore not taking into account fuel swelling and densification during irradiation. The Theoretical Density (TD) is corrected using 95% TD to take into account the porosity and microstructure voids in the fuel ceramics. Furthermore, the fuel density is reduced by smearing the chamfer and dish volumes along the height of the fuel rod. The 188 rods containing UO_2 pellets have a U-235 enrichment of 4.25 wt.% whereas the 16 gadolinia rods have a Gd_2O_3 content of 10.0 wt.% and a U-235 enrichment of 2.0 wt.%. The standard isotopic vector of natural gadolinium is considered as reference isotopic composition. Furthermore, only the U-235 and U-238 isotopes are taken into account for the modeling of the uranium vectors in the initial fuel composition.

The above-mentioned densities and isotopic compositions are the nominal values available for the UO_2 and UO_2–Gd_2O_3 rods in the fuel assembly. To more accurately describe the investigated D05 and E14 rods, batch data available from the fuel manufacturer for these two rods was used rather than the average rod data. Batch-measured densities were used to take into account the proper porosity and voids in the measured fuel rods. The uranium vectors were measured with high precision after enrichment and contain information on the residual U-234 and U-236 components.

3.3. Benchmark definition

Based on the properties and operational history of the fuel rods previously discussed, a benchmark model has been defined. The relevant benchmark specifications are summarized in the next items.

Geometrical modeling. A two-dimensional (2D) representation is used for the full 15 × 15 assembly, and a reflective boundary condition is applied to the outermost boundaries. For the implementation of this representation in three-dimensional (3D) codes, an appropriate layer height in the third dimension is chosen, greater than the neutron free-mean path, with appropriate boundary conditions applied. All rods in the model are depleted individually by taking into account the 1/8 symmetry of the assembly, as indicated in Fig. 2. An equal-volume 16 zones radial meshing is adopted for all gadolinia rods and the measured D05 rod.

Dimensions. All dimensions are assumed to be constant during irradiation. Regarding the application of thermal expansion to (cold) geometrical data, the assembly and rod pitch expansion (due to spacer grid thermal expansion) are accounted for, while the rod dimensions are left unchanged. Rod dimension changes are much more complex and involve other phenomena such as re-densification, solid and gaseous swelling, cracking, fragment relocation (fuel), and creep-down and pellet-cladding mechanical interaction deformation (cladding) so that the net effect is more balanced.

Temperatures. Constant material temperatures are set as follows: 600 K for coolant and cladding; 900 K for the fuel. Notwithstanding the simplification of the coolant temperature, the coolant

density is evaluated according to the coolant pressure and the actual (irradiation-averaged) temperature at the sample elevation based on linear interpolation between inlet and outlet temperatures.

Boron concentration. The boron content in the coolant is considered constant over the irradiation period, at a concentration of 500 ppm, equal to the cycle-averaged value.

Fuel composition and density. A smeared density is used for fuel which accounts for dish and chamfer volumes. Rod-averaged values are used for composition and density of the UO_2 and UO_2–Gd_2O_3 rods in the fuel assembly, whereas batch-specific values are used for the individual D05 and E14 rods.

Power history. The power history is discretized in steps smaller than 1 GWd/t_{HM} and 0.5 GWd/t_{HM} for the D05 and E14 benchmarks, respectively. For the E14 case, a smaller step size was chosen to better account for the fast gadolinium burnout. The system power is normalized to the power of the individual D05 and E14 rods (see Fig. 1).

Burnup and power renormalization. Due to the definition of the quantity "burnup" as the energy released per mass of heavy metal, it is important to know whether so-called secondary energy deposition is taken into account. This second energy deposition comprises the energy deposited by gamma rays coming from (n,γ) reactions in fuel but also in neutron-absorbing isotopes. To overcome this different interpretation of burnup, the power history can be renormalized based on a correct reproduction of the experimental Nd-148 content at the analysis date. This typically requires some iterative procedure in the depletion calculations to match this Nd-148 content with sufficient accuracy. The magnitude of this correction and the effect on the burnup are discussed in Section 5.1.

Decay time. A decay time of 4630 days and 3900 days is considered for the D05 and the E14 rods, respectively. This decay time corresponds to the elapsed time between the end of irradiation and the radiochemical analysis date.

4. Computational models

The benchmark specifications defined in Section 3 served as a guideline for the simulation of the D05 and E14 samples depletion. Although these specifications are unambiguously defined, inherent limitations of the simulation codes and/or further simplifications needed, depending on the code itself or the way depletion calculations are treated, led to differences in implementation. This section summarizes specific implementation approaches applied with the codes used by participants and provides a brief description of the code, to serve further on in understanding any potential impact on the calculation-measurement comparison for the considered nuclides.

4.1. ALEPH

ALEPH2 (Stankovskiy et al., 2020) is a Monte Carlo burnup code developed at SCK CEN, which couples the Monte Carlo particle transport codes MCNP or MCNPX with a deterministic depletion algorithm. The most recent version of ALEPH2 allows the use of two different depletion solvers: the ORIGEN 2.2 (Croff, 1980) solver and the RADAU5 (Hairer and Wanner, 2002) solver. One of the strengths of the ALPEH2 code is its data consistency: the same source of nuclear data is used for particle transport and for the decay data and the energy-group cross section collapsing that feeds the depletion solver. For the current benchmark exercise, ALEPH2 version 2.8 is used, using both the JEFF-3.3 and ENDF/B-VIII.0 nuclear data libraries.

The assembly and depletion regions were modeled using a 3D representation of the 1/4 assembly model, taking advantage of the symmetry of the configuration. Reflective boundary conditions were applied at the model outer boundary. Whereas 28 UO_2 fuel rods in the configuration were represented with no radial zoning, the measured D05 rod was modeled with radial zoning that included 16 concentric equal-volume regions. The gadolinia rods were also radially zoned with 16 rings, leading to a total of 92 different depletion zones in the model. The temperatures and densities were used according to the benchmark definition, without evolution in time, and using a rod-average fuel density.

The irradiation history at sample level was incorporated in the model using depletion steps of less than 1 GWd/t_{HM} (with an average of 0.7 GWd/t_{HM}). The power was normalized to the D05 sample level. The MCNP code was used in KCODE mode, necessary to update the flux spectrum in the depletion zones for each irradiation step. The statistical uncertainty (1–sigma) in the calculated k-eff was 7 pcm (1 pcm = 10^{-5}). A number of 5×10^5 particles per cycle and 200 active cycles were used for MCNP transport calculations. The power history is rescaled to match the experimental value of Nd-148 concentration.

4.2. SCALE

SCALE is a modeling and simulation suite for nuclear safety analysis and design (Wieselquist et al., 2020) that is developed and maintained by ORNL. The computational analyses herein were performed with version SCALE 6.2.2, using the following depletion capabilities:

- The TRITON depletion sequence, which couples one of the neutron transport modules available in SCALE with the ORIGEN depletion and decay code, in an iterative time-stepping manner, to span the irradiation history. In SCALE, one can choose between a deterministic, general geometry, 2D (NEWT), and a 3D Monte-Carlo neutron transport solver (KENO-V.a or KENO-VI). The latter can be run in a multi-group or in continuous-energy mode.
- The Polaris lattice physics code, which was introduced in SCALE 6.2, specifically developed for LWR assembly geometries. It couples a 2D deterministic neutron transport solver that is based on the method of characteristics to evaluate self-shielding and lattice shielding effects, with the ORIGEN code used for depletion calculations.

In this work, depletion simulations with SCALE were performed with each of these three approaches: (1) TRITON/KENO-VI in multi-group mode, (2) TRITON/NEWT, and (3) Polaris. The 252-group built-in cross section library based on ENDF/B-VII.1 evaluated data was used in all these three cases. Internally within TRITON or Polaris, the problem-dependent multi-group neutron flux and cross sections are post-processed at each depletion step and for each depletion material to generate a transition matrix that is used by ORIGEN to calculate the evolution of the nuclide inventories in these materials. The depleted material composition at the end of each depletion step serves as input to the neutron transport solver at the next depletion step.

Each fuel rod material is shielded and depleted (self-shielding and lattice shielding) independently, except for burnable poison rods, for which a radial meshing is applied, where each zone is shielded and depleted independently. The 1/4 symmetry of the assembly configuration has been used to develop a 2D simulation model, with reflective boundary conditions applied to the outermost boundary. As required by the benchmark, the power history of the system is normalized to the D05 sample, using depletion

of steps less than 1 GWd/t_{HM} each. The power history is uniformly rescaled to match the experimental value of Nd-148 concentration.

4.3. VESTA

VESTA 2.2 (Haeck and Dechenaux, 2017) is a Monte Carlo depletion code developed by IRSN, which couples a continuous energy Monte Carlo neutron transport code with a deterministic depletion module. The VESTA 2.2 calculations performed for the REGAL benchmark used the MCNP6 Monte Carlo code and the IRSN PHOENIX depletion module. The nuclear data libraries used for this study are based on ENDF/B-VII.1 and JEFF-3.2 libraries.

The symmetry of the system has been used to develop a 1/8 assembly model in a 3D representation using MCNP6 and based on the benchmark specifications. Reflective boundary conditions were applied to the outermost boundary. All fuel rods are individually depleted assuming a constant power over a time interval. According to the benchmark specifications, the UO_2 rods are modeled as a single zone, except for the investigated rod. Burnable poisons rods and the investigated rod are discretized in a set of 16 equal-volume concentric rings. The simulation uses the benchmark-provided smeared fuel density, all fuel temperatures set at 900 K, and cladding and moderator temperature set at 600 K. The water moderator used in the calculations contains an average boron concentration of 500 ppm, as provided in the benchmark specifications. No time-dependent temperature evolution has been modeled.

The irradiation history is subdivided into depletion steps of 1 GWd/t_{HM}, according to the VESTA validation procedure (Ichou, 2020). The number of particles per cycle and the number of active cycles for the MCNP calculation are determined to ensure statistical errors in the flux of less than 0.1% for every depletion zone. Calibration of the irradiation history on the chosen burnup indicator (or indicators) was applied to assess the burnup of the sample. The sum of Nd-145, Nd-146, and Nd-148 is used as the standard burnup indicator set in this simulation (Haeck et al., 2014). Calibration consists of determining a global renormalization constant to be applied to the irradiation history as a whole. This renormalization constant is determined through iteration until the relative difference between the combined value for the burnup indicators and the target value is less than 0.1%.

4.4. WIMS

WIMS (Lindley et al., 2015) is a general-purpose reactor physics code developed by the ANSWERS British company, which is part of the Jacobs Engineering Group. The code includes deterministic and probabilistic neutron transport solvers that can model 2D and 3D geometries. The calculations for this benchmark were performed with the code version WIMS10 ru0. A 172-group cross section library that used for the benchmark is based on ENDF/B-VII.1 data. This library has been prepared by the code developers with standard modules of NJOY (Macfarlane, 2017). A typical PWR weighting spectrum was used to perform the cross section condensation. In addition to the broad-group data, the library does also contain fine group data for resonant nuclides which have been produced by a set of NJOY modules developed specifically for this purpose.

The WIMS depletion sequence that has been used in the calculation includes the following steps:

1. Calculate materials self-shielded cross Sections (172 groups) with either the equivalence theory or the so-called "subgroup-methods" which is more accurate at the price of extra computational cost (Gibson et al., 2015), the latter being applied for to a limited set of actinides (i.e. U-235 and U-238)
2. Calculate materials broad-group cross Sections (22 groups) using a probabilistic first collision approach on a simplified geometry.
3. Solve the eigenvalue problem for the whole geometry using CACTUS 2D (neutronic solver based on the method of characteristics (Halsall, 1993))
4. Update the nuclide concentrations based on the flux solution calculated at step 3 and the depletion history provided by the user.
5. Return to step 1 until the target burnup has been reached.

The WIMS model that has been developed for the benchmark represents a 2D assembly slice to which reflective boundary conditions have been applied. The burnable zones take into account the 1/8 symmetry, whereas the transport solver operates at the full assembly model. The D05 rod has been divided into 16 concentric zones as required by the benchmark specifications. The other fuel rods were regrouped according to their position within the assembly, each symmetric position being associated with a unique material number or a unique set of materials for the poison rods since they also include the onion-like internal material structure (i.e. 16 concentric equal-volume rings).

The definition of the different materials corresponds to the specifications given in the benchmark, the only deviation being the cladding density which is lower due to the gap which must be homogenized with the cladding to ensure numerical stability.

WIMS allows choosing between two different options for power normalization: the user can either define an average power history (i.e averaged on all fuel materials present in the model) or specify the power of a given material, the power of the other materials being automatically scaled by the code on basis of the incumbent flux solution. The second option is more suitable for the benchmark and was as such applied to model the D05 fuel rod. The entire power history was uniformly rescaled to match the experimental Nd-148 concentration.

5. Analysis results

5.1. Validation and burnup normalization

As stated in the benchmark definition, the power of the system and consequently the burnup is normalized by matching the experimental concentration of the Nd-148 nuclide (or a combined set of Nd nuclides for VESTA). The power normalization is achieved using an iterative approach which is terminated after the first iteration for all the codes except for VESTA which uses multiple iterations. For the D05 calculation, a small reduction of the power normalization of typically 2% is necessary after the first iteration whereas for the E14 calculation a more significant increase of 8% was found to be necessary. The Nd-148 nuclide is a widely used experimental burnup monitor due to its stability, relatively high fission yield, and lack of significant contribution of neutron captures and decays of other nuclides in its transmutation chain. As such, the burnup is referred to as the sample burnup rather than the rod burnup. In Fig. 3 (left), the calculated concentration of the Nd-148 nuclide is plotted as a function of burnup for the D05 sample, for each of the codes. It exhibits a linear behavior as expected, with a similar concentration value of Nd-148 at the end of irradiation being observed among all the codes. Furthermore, it indicates that the combination Nd-145, Nd-146 and Nd-148 nuclides for the power normalization as used in the VESTA calculation does not introduce any bias in the power normalization.

A different behavior is observed for the E14 sample, as can be seen from Fig. 3 (right). Though the power normalization for all the codes is based on the same experimental Nd-148 concentration

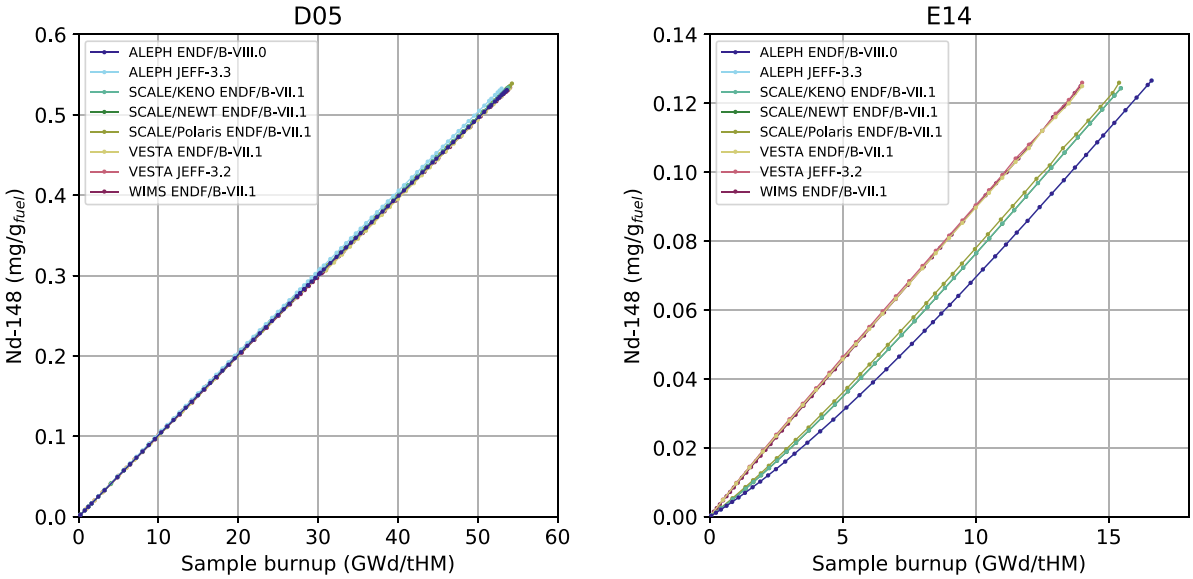

Fig. 3. Evolution of the accumulated Nd-148 concentration as function of the sample burnup for D05 (left) and E14 (right).

and a quasi-linear behavior with burnup for all codes is observed, the final burnup at which the calculation matches the measured Nd-148 varies among the codes. This can be understood in terms of differences in code-specific assumptions or data, in particular related to the contribution of energy release from (n,γ) reactions to the burnup, both in fuel and in the gadolinium isotopes. Given the high cross section for neutron capture (hence their use as a burnable neutron poison) for these Gd nuclides and their high concentration in the gadolinia fuels, the contribution of the energy released from neutron capture reactions in these nuclides to the total energy release is important. WIMS and VESTA do not explicitly attribute any energy from these neutron captures in the burnup whereas ALEPH and SCALE do incorporate such contribution, therefore explaining part of the differences at the end sample burnup value as observed in the plot. A constant recoverable neutron capture energy of 5 MeV per capture is assumed in SCALE for both Gd-155 and Gd-157; whereas a nuclide-dependent capture energy in the range 8–8.5 MeV per capture is applied in ALEPH for these two Gd isotopes. The observed non-linearity reflects the gadolinium burnout rate in the fuel, which will be further discussed in the next section.

5.2. Burnout of gadolinium nuclides

The burnout rate of the gadolinium nuclides was investigated to understand the evolution in time of the infinite multiplication factor for the modeled assembly. For illustrative purposes, the calculated concentration of Gd-155 and Gd-157 as a function of the burnup is shown in Fig. 4 (left) for the E14 sample as calculated with SCALE-NEWT. The burnout rate is high during the first part of the irradiation, up to 8–10 GWd/t$_{HM}$, due to neutron captures, leading to a reduction of two orders of magnitude in nuclide concentration compared to its initial value in non-irradiated fuel. The burnout rate for Gd-157 is higher than that for Gd-155 due to a 4-fold larger neutron capture cross section. Equilibrium is reached for both nuclides at longer irradiation time when there is a balance between removal and production (by means of neutron captures in the abundant Gd-154 and Gd-156 isotopes).

The radial equilibrium profiles for Gd-155 and Gd-157 at the end-of-life are illustrated in Fig. 4 (right). The profiles reflect the neutron transport and self-shielding effects to a high degree. For both Gd-155 and Gd-157, concentrations near the fuel pellet edge are higher due to a higher production rate from captures by Gd-154 and Gd-156 respectively, which in this region are less affected by self-shielding effects. Towards the center of the fuel pellet, the equilibrium concentration reduces for both nuclides. At the center of the fuel pellet, the calculated Gd-155 increases again, likely due to a different behavior in its effective capture cross section compared to that of Gd-157, as function of the self-shielded flux spectrum at the center.

5.3. Infinite multiplication factor evolution

The evolution of the infinite multiplication factor and related reactivity is important for nuclear reactor codes as such calculations are directly used in the baseline core optimizations and safety studies. The infinite multiplication factor is defined at the assembly level. Whereas for nominal UO_2 only assemblies the reactivity decreases almost linearly as a function of burnup (per the linear reactivity model), in this particular case where gadolinia rods are present in the assembly the reactivity evolution is significantly impacted by these rods. Non-linear effects become apparent in this case, as illustrated in Fig. 5 that presents the assembly infinite multiplication factor as a function of the calculated Nd-148 concentration at sample level. The Nd-148 is chosen as an evolutionary parameter here rather than burnup for consistent comparison and to avoid any bias in the burnup definition among the different codes. For each of the two cases shown in Fig. 5, a similar trend is noted (increase to a peak reactivity followed by decrease), which is expected as the fuel assemblies are similar, though differences are noticeable due to the different power histories. During the first part of irradiation, the positive reactivity contribution by the fuel is compensated by the presence of the strong gadolinium absorbers, which will gradually burn out causing a peak in reactivity. Afterward, the reactivity decreases linearly towards the end of irradiation, similar to the behavior of nominal UO_2 fuel assemblies. Differences between the codes can be explained by differences in the gadolinium burnout rates, due to differences in the underlying neutron transport solvers and depletion treatment used with these computational tools.

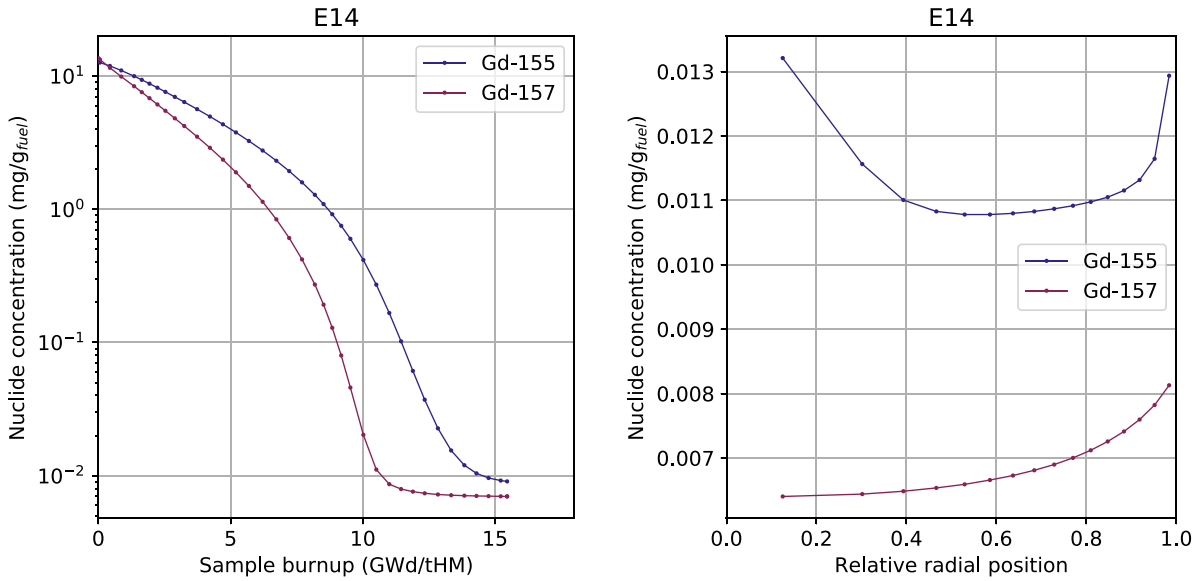

Fig. 4. Evolution of Gd-155 and Gd-157 as function of the burnup (left) and end-of-life radial concentrations (right) for the E14 sample. For illustrative purposes only SCALE-NEWT is shown, other codes yield similar results.

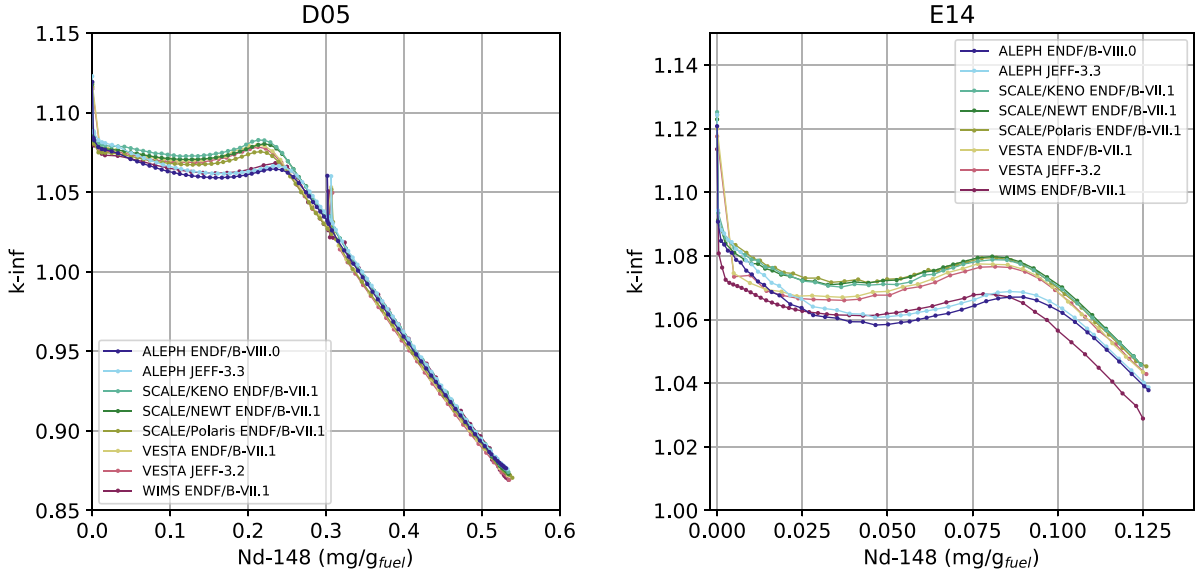

Fig. 5. Evolution of the infinite multiplication factor at assembly level for the D05 calculation (left) and E14 (right).

5.4. Comparison to experimental results

The calculated nuclide concentrations are compared against experimental measurements using a C/E−1 format, where C is the calculated value (per code) and E is the measured or experimental value, both expressed in g/g$_{fuel}$. A correct decay time is taken into account when evaluating the nuclides, as stated in the benchmark definition. Results are graphically represented in Figs. 6 and 7, and tabulated in Tables 3 and 4, respectively for the D05 and E14 samples. Relevant actinides and fission products are reported. The error bar in the plots reflects the experimental uncertainty. It can be seen that, despite the fact that the benchmark was defined to enable common implementation among codes rather than developing a best-estimate model, the majority of the nuclides are predicted within or close to their experimental uncertainty range, with a moderate variation observed among the codes.

Nuclides of the fission product Nd are generally well predicted as expected, given the strong correlation with the burnup normalization. Small residual differences are attributed due to the iterative nature of the power normalization, which is more sensitive for the E14 rod repletion. Nuclides Nd-143 and Nd-145, which are strong neutron absorbers of importance to burnup credit, are well predicted, within 2% of the measurement by all codes considered and in both samples. Cs-137, a strong gamma emitter with an important contribution to the decay heat from pre-disposal management and disposal perspectives and also known as a good burnup indicator, is well predicted by all codes for the D05 sample, within 2% of the experimental value. The systematical overprediction of Cs-137 in the E14 sample by all codes, by 7 to 9%, is coherent with the fact that E14 was a leaking fuel rod, and that part of the Cs was leached out of the rod as indicated from a comparison of the gamma scan (dominated by Cs-137 emissions) to the burnup

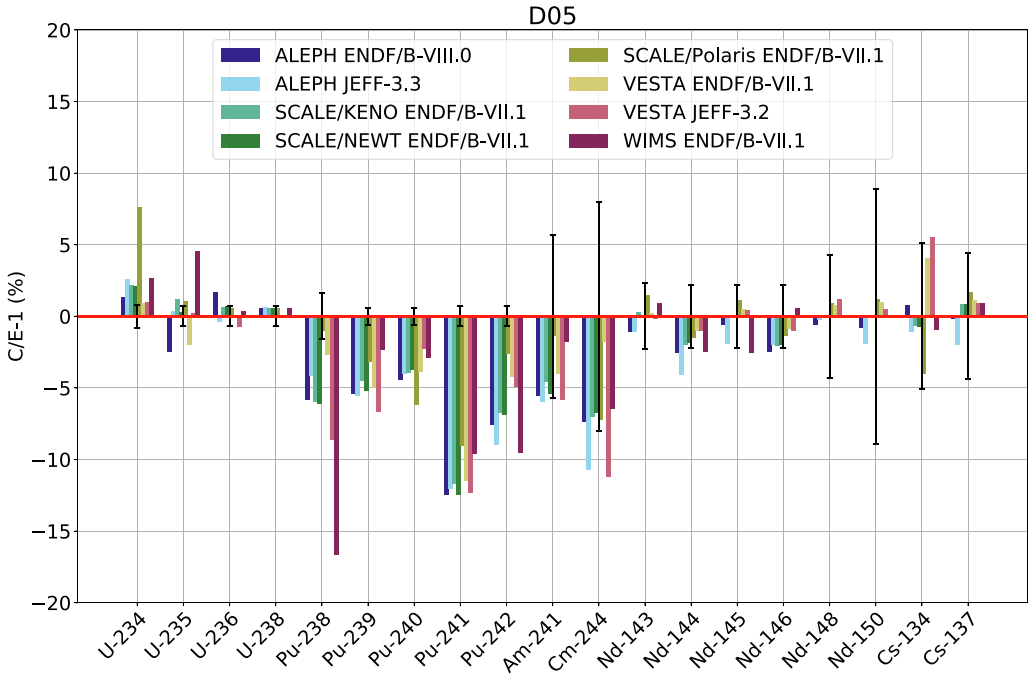

Fig. 6. Comparison of code predictions to experimental measurements for the D05 sample, expressed in percentage as C/E-1 with C the calculated value (per code) and E the experimental value in g/g_{fuel}.

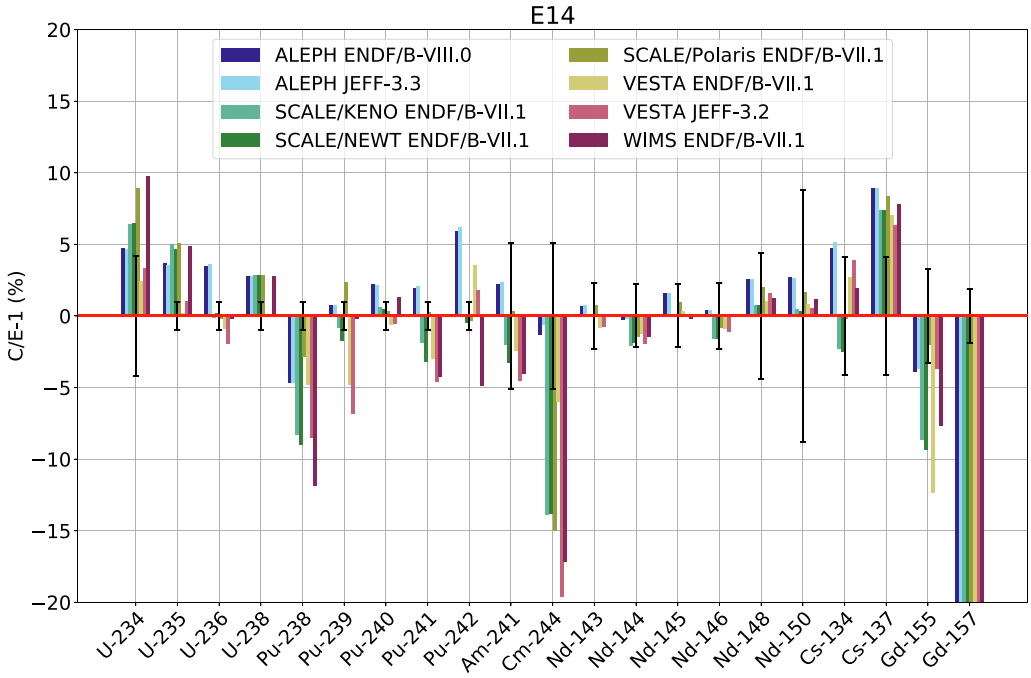

Fig. 7. Comparison of code predictions to experimental measurements for the E14 sample, expressed in percentage as C/E-1 with C the calculated value (per code) and E the experimental value in g/g_{fuel}. Due to the large discrepancy, the C/E-1 value for Gd-157 is outside of the scale shown.

axial profile calculated by the operator. The Cs-134 nuclide, also a strong gamma emitter and significant contributor to decay heat over the first year after discharge from the reactor, is predicted within 5% by all codes in both samples. Note that both Cs-134 and Cs-137 are predicted within the reported measurement uncertainties for these nuclides. The minor actinides Am-241 (nuclide of significant importance to burnup credit and decay heat applications) and Cm-244 (important for decay heat and neutron emission in spent fuel) are predicted within the experimental uncertainty by most of the codes, and a systematic underestimation of Cm-244 is observed for the E14 sample.

Uranium nuclides are generally well predicted in the D05 sample, with the major actinide U-235 being predicted within 2% of the experiment by almost all codes. However, U-235 in the E14 sample is consistently overpredicted up to 5% for almost all codes. Plutonium nuclides are systematically underpredicted for the D05 sam-

Table 3
Comparison of code predictions to experimental measurements for the D05 sample, expressed in percentage as C/E-1 with C the calculated value (per code) and E the experimental value in g/g_{fuel}. The nuclide "Fissile" is the sum of U-235, Pu-239, and Pu-241.

Nuclide	ALEPH	ALEPH	S. KENO	S. NEWT	S. Polaris	VESTA	VESTA	WIMS
	ENDF/B VIII.0	JEFF 3.3	ENDF/B VII.1	ENDF/B VII.1	ENDF/B VII.1	ENDF/B VII.1	JEFF 3.2	ENDF/B VII.1
U-234	1.3	2.6	2.2	2.1	7.7	0.9	1.0	2.7
U-235	−2.5	0.4	1.2	0.3	1.0	−2.0	0.2	4.5
U-236	1.7	−0.4	0.6	0.7	0.6	0.1	−0.7	0.4
U-238	0.6	0.6	0.5	0.5	0.5	0.0	0.0	0.5
Pu-238	−5.8	−4.1	−6.0	−6.1	−1.0	−2.7	−8.6	−16.6
Pu-239	−5.4	−5.5	−4.5	−5.2	−3.2	−5.0	−6.7	−2.3
Pu-240	−4.4	−4.0	−4.0	−3.7	−6.2	−3.9	−2.3	−2.9
Pu-241	−12.5	−12.0	−11.7	−12.5	−9.0	−11.5	−12.3	−9.6
Pu-242	−7.6	−9.0	−6.7	−6.9	−2.7	−4.2	−4.9	−9.6
Am-241	−5.5	−6.0	−4.6	−5.4	−1.4	−4.0	−5.8	−1.8
Cm-244	−7.4	−10.7	−7.0	−6.7	−7.2	−1.8	−11.2	−6.4
Nd-143	−1.1	−1.1	0.3	0.0	1.4	0.2	−0.2	0.9
Nd-144	−2.6	−4.1	−2.0	−1.9	−1.5	−1.0	−1.0	−2.5
Nd-145	−0.6	−1.9	0.0	−0.1	1.1	0.5	0.4	−2.5
Nd-146	−2.5	−2.0	−2.0	−2.0	−1.3	−0.9	−1.0	0.6
Nd-148	−0.6	−0.2	0.0	0.0	0.9	0.8	1.2	0.0
Nd-150	−0.8	−1.9	0.0	−0.1	1.2	1.0	0.5	0.0
Cs-134	0.8	−1.1	v0.6	−0.7	−4.0	4.1	5.5	−0.9
Cs-137	−0.2	−2.0	0.8	0.8	1.7	1.1	0.9	0.9
Fissile	−4.6	−3.3	−2.4	−3.2	−1.7	−4.0	−3.7	0.3

Table 4
Comparison of code predictions to experimental measurements for the E14 sample, expressed in percentage as C/E-1 with C the calculated value (per code) and E the experimental value in g/g_{fuel}. The nuclide "Fissile" is the sum of U-235, Pu-239, and Pu-241.

Nuclide	ALEPH	ALEPH	S. KENO	S. NEWT	S. Polaris	VESTA	VESTA	WIMS
	ENDF/B VIII.0	JEFF 3.3	ENDF/B VII.1	ENDF/B VII.1	ENDF/B VII.1	ENDF/B VII.1	JEFF 3.2	ENDF/B VII.1
U-234	4.7	4.6	6.4	6.4	8.9	2.4	3.3	9.7
U-235	3.7	3.5	5.0	4.6	5.1	0.2	1.0	4.9
U-236	3.4	3.6	−0.1	0.1	−0.1	−0.9	−1.9	−0.2
U-238	2.8	2.8	2.8	2.8	2.8	0.0	0.0	2.8
Pu-238	−4.7	−4.6	−8.3	−8.9	−2.8	−4.8	−8.5	−11.8
Pu-239	0.7	0.7	−0.8	−1.7	2.3	−4.8	−6.8	−0.2
Pu-240	2.2	2.1	0.6	0.5	0.3	−0.6	−0.5	1.3
Pu-241	1.9	2.1	−1.9	−3.1	0.2	−3	−4.6	−4.2
Pu-242	5.9	6.2	0.0	−0.5	−0.3	3.5	1.8	−4.9
Am-241	2.2	2.4	−2	−3.3	0.3	−2.4	−4.5	−4
Cm-244	−1.3	−0.6	−13.8	−13.8	−15	−6	−19.6	−17.2
Nd-143	0.7	0.7	0.0	−0.1	0.7	−0.8	−0.7	0.1
Nd-144	−0.2	−0.2	−2.1	−1.9	−1.4	−1.2	−1.9	−1.4
Nd-145	1.6	1.6	0.0	0.0	0.9	0.3	0.1	−0.1
Nd-146	0.4	0.4	−1.6	−1.6	−0.8	−0.9	−1.1	0.1
Nd-148	2.5	2.5	0.7	0.7	2	.01	1.6	1.2
Nd-150	2.7	2.6	0.5	0.3	1.6	0.8	0.5	1.1
Cs-134	4.7	5.1	−2.3	−2.5	−0.1	2.7	3.9	1.9
Cs-137	8.9	8.9	7.4	7.4	8.3	7	6.3	7.8
Gd-155	−3.9	−3.7	−8.6	−9.3	−2.0	−12.3	−3.7	−7.6
Gd-157	−61.7	−58.7	−63.5	−64.2	−61.0	−65.8	−59.9	−41.7
Fissile	2.6	2.5	2.9	2.3	4.0	1.1	0.8	2.9

ple but within the experimental uncertainty range for the E14 sample, indicating a bias dependency with burnup. At high burnup where the plutonium content is much higher than at low burnup, the plutonium fission is significant and any bias (e.g. benchmark-wise or neutronic-data related) in the plutonium modeling, which is known to be sensitive to the neutron spectrum, would manifest to a higher degree than at lower burnup.

The total fissile inventory (see Tables 3 and 4) is overpredicted by all the codes with 1–4% for the D05 sample but underpredicted with 1–4% for the E14 sample. Within the current benchmark calculations, there is no definitive explanation for the causes of the observed differences between calculated and measured nuclide concentrations. Sensitivity studies and best-estimate benchmark models, as planned for future efforts, are necessary to give more insights in the causes for these observed differences. A first step would consist in evaluating the effect of the experimental uncertainty on the power normalization by Nd-148.

Notably, both Gd-155 and Gd-157 are systematically underestimated by all codes. The Gd-155 nuclide is predicted within an acceptable accuracy considering the experimental uncertainty. On the other hand, Gd-157 is largely underpredicted, in the 40–60% range. Note that the concentration of these nuclides at end-of-life is low (see Fig. 4) and that the calculated values may be impacted by uncertainties due to computational assumptions

(e.g. modeling of the boron curve) and nuclear data. The cause of such uncertainties could be searched for by a series of sensitivity studies or a best-estimate model.

6. Conclusions

The first phase of the REGAL international program has provided valuable high-quality experimental data to fill in existing gaps in the database of nuclide inventories for spent fuel that can be used as a validation basis for computational tools and nuclear data. REGAL specifically adds data to investigate the impact of burnup gradients at rod extremities for characterization of modern, high duty, nuclear fuel and the impact of gadolinium as a burnable neutron poison. Preliminary evaluations of measurements performed for two fuel samples during the first phase of the program are discussed in this paper. The computational assessments presented here are based on an initial benchmark that was designed to serve as a consistent investigation basis for the experimental data evaluation using multiple computational tools and nuclear data. The primary goal of this assessment was to identify any improvements that would be necessary to develop adequate best-estimate models, as well as to identify any unexpected behavior in the comparison calculation-experiment for the considered nuclides. The latter would be instrumental in pointing out potential gaps in the nuclear data used in the simulation or in the level of detail necessary in a best-estimate model, as well as in indicating qualitative impacts of various modeling approximations used with different codes.

Both measured samples discussed here were selected from fuel rods irradiated in PWR fuel assemblies that contained gadolinia rods as integral burnable absorbers. The measured UO_2–Gd_2O_3 sample is unique, having the highest Gd_2O_3 loading (10 wt.%) and the lowest burnup (relevant for peak reactivity) among all gadolinia samples for which destructive assay data are available in the open literature. The nuclide concentrations calculated for the UO_2 sample are generally in good agreement with the measured values and show differences that are likely due to the differences in the computational method (Monte Carlo-based depletion vs. deterministic-based depletion) and various nuclear data used in the simulations (JEFF-3.2, JEFF-3.3, ENDF/B-VII.1, ENDF/B-VIII.0). In the calculation-measurement comparison, a good agreement was found for the Gd-155 nuclide whereas a consistent underprediction of the Gd-157 nuclide concentration irrespective of the code and nuclear data involved was noted, with calculated values departing by 40–60% from the measured value. This could indicate potential deficiencies in the cross sections of isotopes involved in the evolution chain for this nuclide, as well as a need for using an adequate value for the energy release (Q) from decay for this specific nuclide. Another potential cause of this discrepancy, to be further investigated, is a currently used simplified approach for the modeling of the boron curve or other operating parameters for the gadolinia rod.

Efforts in the next phase of the REGAL program will include, in addition, cross-check measurements leading to improvements in the experimental uncertainties, concerted sensitivity, and uncertainty studies to determine the bias and uncertainty associated with the computational models and assumptions.

CRediT authorship contribution statement

J. Eysermans: Investigation, Writing - original draft, Writing - review & editing, Visualization, Methodology, Formal analysis. **M. Verwerft:** Project administration, Methodology, Conceptualization. **K. Govers:** Investigation, Methodology, Conceptualization. **R. Ichou:** Investigation. **G. Ilas:** Investigation, Writing - original draft, Writing - review & editing. **U. Meryturek:** Investigation, Writing - original draft, Writing - review & editing. **N. Messaoudi:** Investigation. **P. Romojaro:** Investigation. **N. Slosse:** Investigation.

Declaration of Competing Interest

The authors declare that they have no known competing financial interests or personal relationships that could have appeared to influence the work reported in this paper.

Acknowledgements

This research was partly sponsored under the General Framework Agreement ENGIE – SCK CEN 2013–2017 (project 7300).

References

Boulanger, D., Lippens, M., Mertens, L., Basselier, J., Lance, B., 2004. High Burnup PWR and BWR MOX Fuel Performance: A Review of BELGONUCLEAIRE Recent Experimental Programs, ANS International Meeting on LWR Fuel Performance, Orlando, FL, USA, September 19–22.

Baeten, P., et al., 2002. The Burnup Credit Experimental Programme REBUS,-Practices and Developments in Spent Fuel Burnup Credit Applications, Proceedings of a Technical Committee Meeting, Madrid, April 22–26, IAEA-TECDOC-1378.

Hesketh, K., Rossiter, G., Largenton, R., Puide, M., 2020. Burnable Poison-Doped Fuel, Comprehensive Nuclear Materials. Elsevier, Oxford, pp. 106–124.

Manzel, R., Dorr, W., 1980. Manufacturing and irradiation experience with UO2-Gd2O3 fuel. Am. Ceram. Soc. Bull. 59, 601–603.

OECD-NEA, 2017. SFCOMPO 2.0: Database of Measured Isotopic Concentrations of Spent Nuclear Fuel, with Operational Histories and Design Data,https://www.oecd-nea.org/sfcompo.

Michel-Sendis, F., et al., 2017. SFCOMPO-2.0: An OECD NEA database of spent nuclear fuel isotopic assays, reactor design specifications and operating data. Ann. Nucl. Energy, 110, 779–788.

OECD-NEA, 2011. Spent Nuclear Fuel Assay Data for Isotopic Validation - State-of-the-art Report, OECD/NEA, report NEA/NSC/WPNCS/DOC(2011)5.

Govers, K., Dobney, K., Gysemans, M., Verwerft, M., 2015. Technical scope of the REGAL base program, revision 1.2, SCK CEN-ER-110.

Croff, A.G., 1980. User 's Manual for the ORIGEN2 Computer Code, ORNL/TM-7175 Tennessee.

Stankovskiy, A., et al., 2020. ALEPH: A Monte Carlo Depletion Code - Version 2.8, SCK CEN report R-7449.

Hairer, E., Wanner, G., 2002. Solving ordinary differential equations II, Stiff and Differential-Algebraic problems, 2nd Edition, Springer Series in computational mathematics, Springer-Verlag, 2002, corrected second printing.https://doi.org/10.1007/978-3-642-05221-7.

Haeck, W., Dechenaux, B., 2017. VESTA User's Manual – Version 2.2.0, IRSN Report PSN-EXP/SNC/2017-00251.

Wieselquist, W.A., Lefebvre, R.A., Jessee, 2020. M.A. SCALE Code System, ORNL/TM-2005/39, Version 6.2.4, Oak Ridge National Laboratory, Oak Ridge, TN.

Ichou, R., 2020. Validation of VESTA 2.2.0 - Volume 1: Methodology and overview of results, IRSN PSN-EXP/SNC/2020-00269.

Haeck, W., Cochet, B., Bernard, F., Tymen, A., 2014. Experimental validation of VESTA 2.1, Proceedings of Supercomputing in Nuclear Applications and Monte Carlo International Conference (SNA+MC) doi:10.1051/snamc/201403603.

Lindley, B.A., et al., 2015. Release of WIMS10: A Versatile Reactor Physics Code for Thermal and Fast Systems, Proceedings of ICAPP 2015, Nice, France.

Macfarlane, R. et al., 2017. The NJOY Nuclear Data Processing System. Version 2016. https://doi.org/10.2172/1338791.

Gibson, N., Smith, K., Forget, B., 2015. Simple benchmark for evaluating self-shielding models, Proceedings of Mathematics and Computations, Supercomputing in Nuclear Applications and Monte Carlo International Conference (M&C+SNA+MC).

Halsall, M.J., 1993. Neutron transport in WIMS by the characteristics method, Trans. Am. Nucl. Soc.